Anal. Bioanal. Electrochem., Vol. 12, No. 6, 2020, 810-827

Analytical & Bioanalytical Electrochemistry

2020 by CEE
www.abechem.com

Full Paper

Simultaneous Determination of Hg(II), Cd(II), Pb(II) and Zn(II) by Anodic Stripping Voltammetry using Modified Carbon Paste Ionic Liquid Electrode

Ashkan Faridan, Manochehr Bahmaei*, and Amirabdolah Mehrdad Sharif

Department of Analytical Chemistry, Faculty of Chemistry, Islamic Azad University, North Tehran Branch, Tehran, Iran

*Corresponding Author, Tel.: +98 9121488481

E-Mail: M_bahmaei@iau-tnb.ac.ir

Received: 8 May 2020 / Received in revised form: 7 June 2020 / Accepted: 15 June 2020 / Published online: 30 June 2020

Abstract- In the presented study, CuO-CoO-MnO/SiO_2 nanocomposite was synthesis by Cu(II), Co(II), Mn(II), with 1:1:1 mole ratio and Tetraethyl orthosilicate. azo–azomethine 1-(3-imino-4-hydroxophenylazo-4-nitrobenzene)-4-methyl phenol (L) was synthesized and used as a ligand for capturing the metal ions. Also, 1-butyl-1-methylpyrrolidinium bis(trifluoromethylsulfonyl)imide was applied as the ionic liquid in order to increase the conductivity of the electrode. The nanomaterials were investigated using Fourier-transform infrared spectroscopy (FTIR) and scanning electron microscopy (SEM); SEM image shows a homogeneous CuO-CoO-MnO/SiO_2 nanocomposite, with an average particle size distribution of 40 nm. Also, the electrochemical characterization of L/CuO-CoO-MnO/SiO_2/IL/CPE was checked by electrochemical impedance spectroscopy (EIS) and cyclic voltammetry (CV) techniques. The modification of carbon paste electrode applied to determination of some heavy metal ions include Hg(II), Cd(II), Pb(II) and Zn(II) by square wave anodic stripping voltammetry (SWASV), for the first time. The linear range for determination of analytes in optimized condition was obtained as Hg: 0.0007-0.21 and 0.21-27 µM, Cd: 0.0007-0.21 and 0.21-27 µM, Pb: 0.0009-0.23 and 0.23-27 µM, Zn: 0.001-0.25 and 0.25-27 µM. Also, the detection limits for Hg(II), Cd(II), Pb(II) and Zn(II) were calculated to be 3.019×10^{-4}, 3.445×10^{-4}, 2.407×10^{-4} and 5.134×10^{-4} µM, respectively. Finally, the sensor was successfully used for the measurement of the analytes in Tap water and River water samples with recoveries ranging between 98.1% and 102.7%. Also, the obtained results accorded very well with those obtained by atomic absorption spectroscopy (AAS) that corroborated the accuracy and validity of the proposed method.

Keywords- Electrochemical Determination; Heavy metal ions; Sensor; CuO-CoO-MnO/SiO_2

1. INTRODUCTION

Heavy metals ions such as Zinc, Cadmium, Lead, and Mercury ions are extremely harmful pollutants in the living organisms in aquatic ecosystems owing to their toxicity and even low concentrations [1-3]. The amount of these heavy metal ions have increased dramatically in the environment due to the several industrial activities such as paint and metallurgical. Besides, these ions are non-biodegradable, so pile up in the biosphere [4].

Hg(II) is applied in chemical, electrical industrials, and medicine [1]. Although a trace amount of Hg(II) is present in our foods, a high level of it can be harmful to the human body. Overdosage of Hg(II) can cause anxiety, depression, irritability, damaging the lining and kidney, memory problems, numbness, pathologic shyness and tremors [4, 5].

Cd(II) one of the material are using in batteries and pigments industrials, which the high dosage of this chemical element causes raise blood pressure and kidney disease [6]. Pb(II), which enters the environment through wastewater (industrial and agricultural), would cause several terrible diseases, for example, kidney disease, cancer and coma [7]. Zn(II) is an essential nutrient which does not naturally produce zinc in the body. It aids growth, skin health, and also has a vital role in DNA synthesis and immune function [8]. Although Zn(II) deficiency is harmful, its high dosage can also ultimate adverse side effects such as nausea, headaches, reduced immune function and diarrhoea [9]. The World Health Organization has declared the highest allowable average concentration of Hg(II), Cd(II), Pb(II) and Zn(II) in drinking water is 6 ppb, 3 ppb, 3 ppb and 5 ppm, respectively [10].

Therefore, measuring these heavy metals by a fast, selective, sensitive, and straightforward analytical method in the environment is urgently necessary to ameliorate the quality of human life.

There are several approach for measuring the heavy metal ions, for example, laser-induced breakdown spectroscopy [11], AAS [12], and inductively coupled plasma atomic emission spectroscopy [13].

The mentioned methods are time-consuming, with complicated procurement steps and also the comparatively costly; however, the advantages of these methods can be sensitivity and accuracy of the method. The disadvantage of the methods restricts their usages to the measurement of analytes [14, 15].

In recent years electrochemical methods have been used as a good procedure to the measurement of many drugs, biomolecules, heavy metals ions and other compounds [16, 17]. Some of the advantages of electrochemical methods are affordable, sensitive, selective and high-speed analysis, with comparatively simple tools, which are the reason for many usages in the researches [18, 19].

Among electrochemical methods, different voltammetric and potentiometric techniques have been mostly used in pharmaceutical and environmental analyses [20]. One of the best voltammetric methods for trace determination of ions is square wave anodic stripping

voltammetry (SWASV) due to analysis speed, low detection limits, good selectivity and high sensitivity [21].

The working electrode and sensing layer can affect the amount of deposited analyte significantly and as a consequence, the sensitivity of SWASV method. Carbon paste electrodes (CPEs) is one of the best choices for using in these methods due to rapid and comfortable preparation, easy modification, ease obtaining a new reproducible surface, porous surface and low price in comparison to other electrodes [21-24].

In order to modify the matrix of CPEs, several procedures have been reported, including the use of carbon-based materials, nanoparticles and nanocomposites, ligands [21, 25].

One of the best procedure to improve the electrochemical sensor performance is using nanoparticles and nanocomposite for the preparation of the sensing layer [26-30]. In electrochemical applications of metal-oxide nanoparticles, they provide several special functions, such as electrocatalytic activity and betterment of conductivity [31].

Copper oxides (CuO), as the transition metal oxides and p-type semiconductors, have specific properties such as nontoxicity and environmentally friendly, stability, low cost, and nontoxicity. This type of semiconductors are applied in solar cell, supercapacitors and lithium-ion batteries, and is an appropriate choice for electrochemical applications [32, 33]. Cobalt monoxide (CoO) nanoparticle is widely used in various instruments such as lithium-ion batteries, gas sensing, and electrochemical devices due to their catalytic, and magnetic [34]. Due to specific physical and chemical properties of Manganese oxides (MnO), it has been considered by many researchers in catalysis, biosensor, and energy storage fields [35]. Silica (SiO_2) has attractive features adsorption capacity, acid/base properties, thermal stability which introduce it as a candidate for use in electrochemical sensor and especially for the accumulation of analytes. The surface of SiO_2 can be modified by various functional groups or nanoparticles, leading to improve their surface properties [36].

Nanocomposites have the properties of components and also a new feature due to the synergetic effect. Among new nanocomposites, double semiconductor oxides have received much attention because of its electronic properties [37]. So the CuO-CoO-MnO/SiO_2 was synthesis to improve the electrocatalytic activity and use for modification of CPE.

A problem in the simultaneous measuring of heavy metals in SWASV method is overlapping of peaks which may occur in the comparatively narrow potential range where heavy metals involved in the redox reaction. One way to solve this problem is the modification of electrodes by using a ligand which can form a complex with the heavy metals. We used an azo–azomethine 1-(3-imino-4-hydroxophenylazo-4-nitrobenzene)-4-methyl phenol (L) as which can form complexes with Hg(II), Cd(II), Pb(II) and Zn(II) [38].

Ionic liquids (ILs) which are classified as a green material, has attracted much attention in electrochemistry filed owning to high stability (chemical and thermal), low vapor pressure, hydrophobicity, low charge transfer resistance (R_{ct}) and wide electrochemical windows. So it

is the best candidate for replacing with non-conductive organic binders which used in CPEs to increase the electron transfer rate, sensitivity and decrease fouling [39, 40].

The main aim of the presented research was to the synthesis of CuO-CoO-MnO/SiO_2 nanocomposite and mixed with an IL and azo-azomethine ligand for modification of bare CPE as a sensing layer. The CuO-CoO-MnO/SiO_2 nanocomposite was investigated by SEM, and FTIR, in addition, CV and EIS was used for checking the electrochemical performance of L/CuO-CoO-MnO/SiO_2/IL/CPE. Under optimum condition, L/CuO-CoO-MnO/SiO_2/IL/CPE illustrates high activity and selectivity for simultaneous and individual measurement of Hg(II), Cd(II), Pb(II) and Zn(II); also it was applied monitoring of the target analytes concentration in different real samples with success.

2. EXPERIMENTAL

2.1. Chemicals and apparatus

All reagents and materials in this study were of analytical grade and were used without any further purification. The raw materials for the synthesis of CuO-CoO-MnO/SiO_2 composite, include Tetraethyl orthosilicate ($Si(OC_2H_5)_4$), cupric acetate, manganese acetate, cobalt acetate, ethanol, HCl and 1-butyl-1-methylpyrrolidinium bis(trifluoromethylsulfonyl) imide (IL), ammonium hydroxide and Hg(II), Cd(II), Pb(II) and Zn(II) (chloride or nitrate) were bought from Merck Company and applied without further refinement. 1-(3-formyl-4-hydroxophenylazo-4-nitrobenzene), 4-methyl-2-aminophenol and dichloromethane were purchased from Sigma-Aldrich and used in synthesizing of the ligand.

Aqueous solutions were produced using deionized water. Britton-Robinson universal buffer solution (B-R buffer solution) was produced by mixing 0.04 M boric acid, 0.04 M acetic acid and 0.04 M phosphoric acid, and applied for adjusting the pH of solutions and as supporting electrolyte.

The electrochemical tests were performed in the ambient temperature by Autolab electrochemical system (302 N, Utrecht, Netherlands) in a conventional three-electrode system including Ag/AgCl/KCl (3 M) electrode, modified and unmodified GCE, Pt wire as a reference electrode, working electrode and the counter electrode, respectively. The Metrohm pH meter instrument (model 713-Switzerland) was used for checking the solution pH. SEM images were taken using an SEM (SEM-EDX, XL30, Philips Netherland). FTIR spectra were procured by a Perkin-Elmer spectrophotometer (Spectrum GX), and XRD patterns were investigated by an XRD (38066 Riva, d/G.Via M. Misone, 11/D (TN) Italy) at room temperature.

2.2. Synthesize of nanomaterials and assemble modified electrodes

For the preparation of CuO-CoO-MnO/SiO_2, the aqueous solutions of Cu(II), Co(II) and

Mn(II), with 1:1:1 mole ratio, were produced by dissolving the acetate salts of metals in deionized water. Tetraethyl orthosilicate, deionized water and ethanol (1:4:8 mol) were mixed at 50 ^{o}C by a magnetic stirrer for 30 min to make homogeneous silica sol. The metal ions solution and homogeneous silica sol were mixed, and the solution pH was adjusted to 3 by addition of 1.2 M HCl. Then to form composite wet gels, pH value was adjusted to 4 by addition of 2.5 M aqua ammonia. The wet gels were exchanged with ethanol twice and then aged in ethanol solvent for 3 days to increase gel firmness, then, it was dried by hot supercritical drying technique at 243 ^{o}C/6.5 MPa for 3 h followed by venting of ethanol gas over 2 h. The prepared nanocomposite was transferred in a furnace and heat-treated at 500 °C in air for 3 h [41].

In order to prepare L, the solution of 500 mg 1-(3-formyl-4-hydroxophenylazo-4-nitrobenzene) in 30 ml ethanol (a) and 22.6 mg 4-methyl-2-aminophenol in 15 ml ethanol (b) was prepared. The solution (a) was added dropwise and slowly to the solution (b), and the obtained mixture was refluxed for 3 h. The mixture was centrifuged, and the red-brown powder was separated and washed twice by ethanol. For getting the high purity product, the obtained red-brown powder was recrystallized in dichloromethane/ethanol and dried [38].

CPEs were constructed with the usual method; summarily, the graphite powder and paraffin oil as the binder (75:25 w/w %) were blended in a mortar using a pestle. For preparing L/CPE, 10% w/w of the synthesized L was well blended with the graphite powder; after that, the mixture was mixed with paraffin oil to obtain a homogeneous paste which the percent by weight of components in the paste was 10:65:25 w/w% for the modifier, graphite powder, and paraffin, respectively. For the construction of L/IL/CPE, the total amount of paraffin oil was replaced with the IL.

To prepare the L/CuO-CoO-MnO/SiO_2/IL/CPE, L, graphite powder and CuO-CoO-MnO/SiO_2 were mixed in an adequate volume of dichloromethane by a magnetic stirrer for 5 h then the mixture dried in vacuum at ambient temperature for 6 h. The IL was added to the mixture to form a homogeneous paste which has 25, 8, 10, 57 % IL, L, CuO-CoO-MnO/SiO_2 and graphite powder, respectively. It should be noted that in this way the reproducibility has increased significantly. Finally, the modified CPEs were constructed by packed each well-mixed paste into the piston-driven carbon paste electrode holder in such a way that all air bubble between layers come out. In order to the renewal of the sensing layer of CPEs, they scrape out with a soft paper.

3. RESULTS AND DISCUSSION

3.1. Investigation of prepared nanocomposites

The FTIR spectra of the synthesized CuO, CoO, MnO, SiO_2 nanoparticles and CuO-CoO-MnO/SiO_2 nanocomposite were appraised, and the consequence is represented in Fig. 1a.

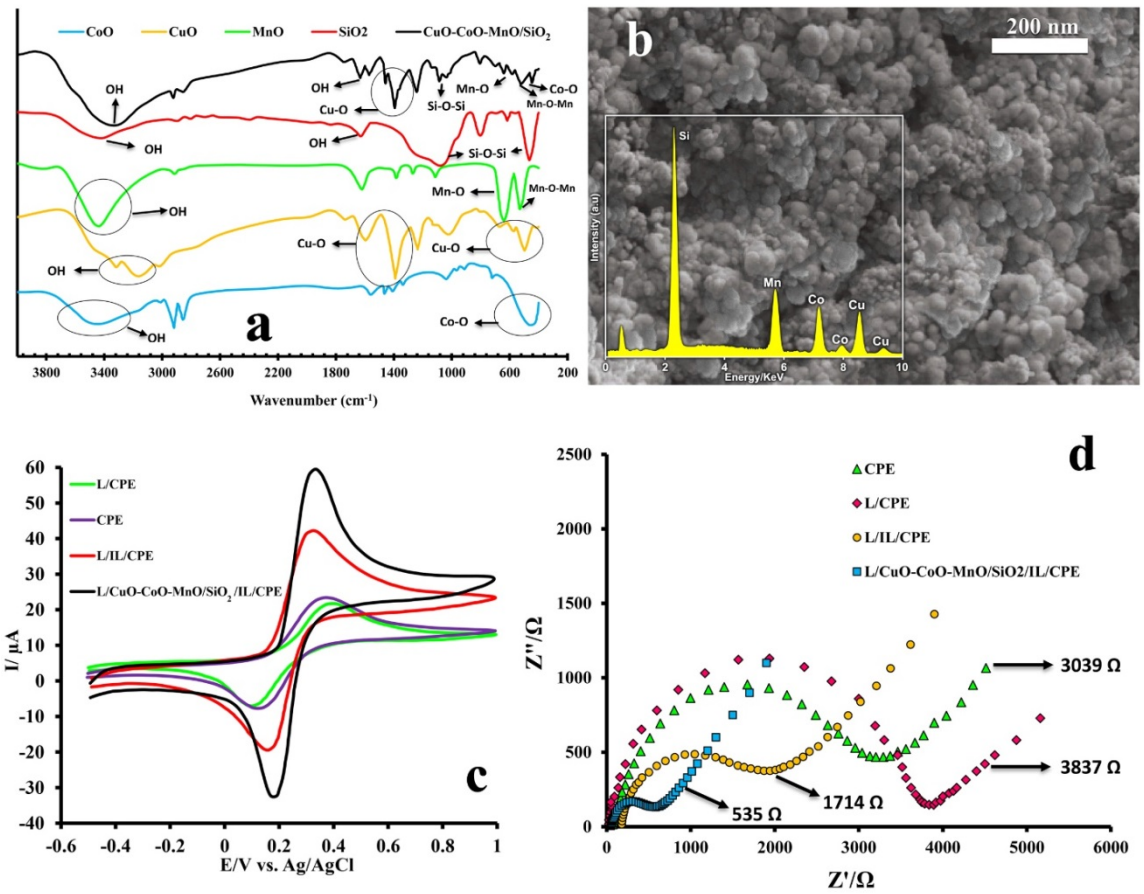

Fig. 1. (a) FT-IR spectra of synthesized CoO, CuO, MnO, SiO_2 and CuO-CoO-MnO/SiO_2; (b) SEM image of CuO-CoO-MnO/SiO_2 (Inset: EDS spectrum of CuO-CoO-MnO/SiO_2 nanocomposite); (c, d) The CVs and Nyquist plots of CPE, L/CPE, L/IL/CPE, and L/CuO-CoO-MnO/SiO_2/IL/CPE in 5 mM $[Fe(CN)_6]^{3-/4-}$ in 1.0 M KCl at a scan rate of 100 mVs^{-1}

The spectrum of CuO depicts absorption peaks at 3315 cm^{-1}, which corresponds to O−H stretching related to water present, the absorption peaks between 1400 to 1600 cm^{-1} are pertinent to the Cu-O asymmetrical and symmetrical stretching, 498 cm^{-1} (stretching of Cu−O), 584 and 668 cm^{-1} which demonstrated the formation of the CuO nanoparticles [42]. The FTIR spectrum of CoO illustrates peaks at 463 and 718 cm^{-1}, which is related to the stretching vibrations Co-O bonds. The absorption peak at 3448 cm^{-1} corresponds to O-H stretching vibrations [43]. The FTIR spectrum of MnO shows specific peaks at 633 cm^{-1} (stretching vibration of Mn-O) and 570 cm^{-1} (stretching vibration of Mn-O-Mn), and 2910 and 3435 cm^{-1} (stretching vibration of O-H) which indicates the synthesis of CoO nanoparticles [35]. For SiO_2 sample, the absorption peak at 1075 and 461 cm^{-1} corresponds to the Si-O-Si asymmetric stretching and bending vibrations. The peaks at 3427 and 1628 cm^{-1} are attributed to –OH groups of synthesis SiO_2 [44]. Besides, the spectrum related to CuO-CoO-MnO/SiO_2 nanocomposite shows specific absorption peaks of CuO, CoO, MnO, SiO_2

nanoparticles, which demonstrate the synthesis of the CuO-CoO-MnO/SiO_2. Fig. 1b represents the SEM image of homogeneous and porous CuO-CoO-MnO/SiO_2 nanocomposite, with an average particle size of 40 nm. Insert of Fig. 1b shows the EDS spectrum and exhibits the presence of Cu, Si, Mn, and Co elements.

3.2. Electrochemical characterization of the constructed electrodes by CV and EIS

Fig. 1c represents the CVs of the bare CPE, L/CPE, IL/L/CPE and L/CuO-CoO-MnO/SiO_2/IL/CPE using a solution of 5.0 mM $[Fe(CN)_6]^{3-/4-}$ in the presence of 1.0 M KCl. The results illustrate that the oxidation peak current (I_{pa}) and the peak potential separation (ΔE_P) have changed by variation of modifiers. At the surface of CPE, the using probe represents broad and weak oxidation and reduction peaks with I_{pa}= 10 μA and ΔE_P=0.232V. Once the L was added to the matrix of the sensing layer, the ΔE_P has increased (ΔE_P =309 Ω) with a low diminution in the oxidation and reduction currents in comparison with CPE. The electron-transfer rate reaction of $[Fe(CN)_6]^{3-/4-}$ had boosted when the IL was added to L/CPE, which is due to the high conductivity of using IL compared to paraffin.

The L/CuO-CoO-MnO/SiO_2/IL/CPE illustrates a symmetric oxidation and reduction peaks with the lowest ΔE_P=164 mV and the highest I_{pa}= 39 μA which is 3.9, 4.33 and 1.7 times bigger than those of bare CPE, L/CPE and IL/L/CPE, respectively. The obtained data suggest that the electrical conductivity and reaction reversibility of this sensor was improved by the simultaneous attendance of CuO-CoO-MnO/SiO_2 nanocomposite and IL.

The interfacial charge transferability of the CPE, L/CPE, IL/L/CPE and L/CuO-CoO-MnO/SiO_2/IL/CPE was checked by EIS analysis in 5.0 mM $[Fe(CN)_6]^{3-/4-}$ in the presence of 1.0 M KCl and the results are shown in Fig. 1d.

The semicircle in the Nyquist plot is directly proportional to R_{ct}. The CPE shows the R_{ct} approximately 3039 Ω. By addition of L to CPE structure, the R_{ct} has increased to 3837 Ω, suggesting that L insulated the surface of CPE and made an interfacial charge transfer inaccessible.

The IL decreases the electron-transfer resistance of L/CPE, and the Rct value decreased to 1714 Ω, which is due to the high conductivity of IL in comparison to paraffin. The best conductivity and lowest electron-transfer resistance were achieved when IL and CuO-CoO-MnO/SiO_2 nanocomposite were used simultaneously (535 Ω), which is owing to the high conductivity of IL and CuO-CoO-MnO/SiO_2, the larger surface area and unique catalytic ability of CuO-CoO-MnO/SiO_2 nanocomposite.

3.3. The electrochemical response of the electrodes for the determination of Hg(II), Cd(II), Pb(II) and Zn(II)

The voltammetric behaviour of 5 μM Hg(II), Cd(II), Pb(II) and Zn(II) in B-R buffer solution pH=3.5, accumulation time= 180 s and accumulation potential= -1.15 V vs.

Ag/AgCl at the surface of bare CPE, L/CPE, IL/L/CPE and L/CuO-CoO-MnO/SiO_2/IL/CPE were investigated by SWASV techniques, and the result is depicted in Fig. 2a. There is very weak oxidation peaks for Hg(II), Cd(II), Pb(II) and Zn(II) was observed at the surface of CPE in the potential range of -1.3 – 0.5 V vs. Ag/AgCl, which can be owning to high charge transfer resistance of CPE.

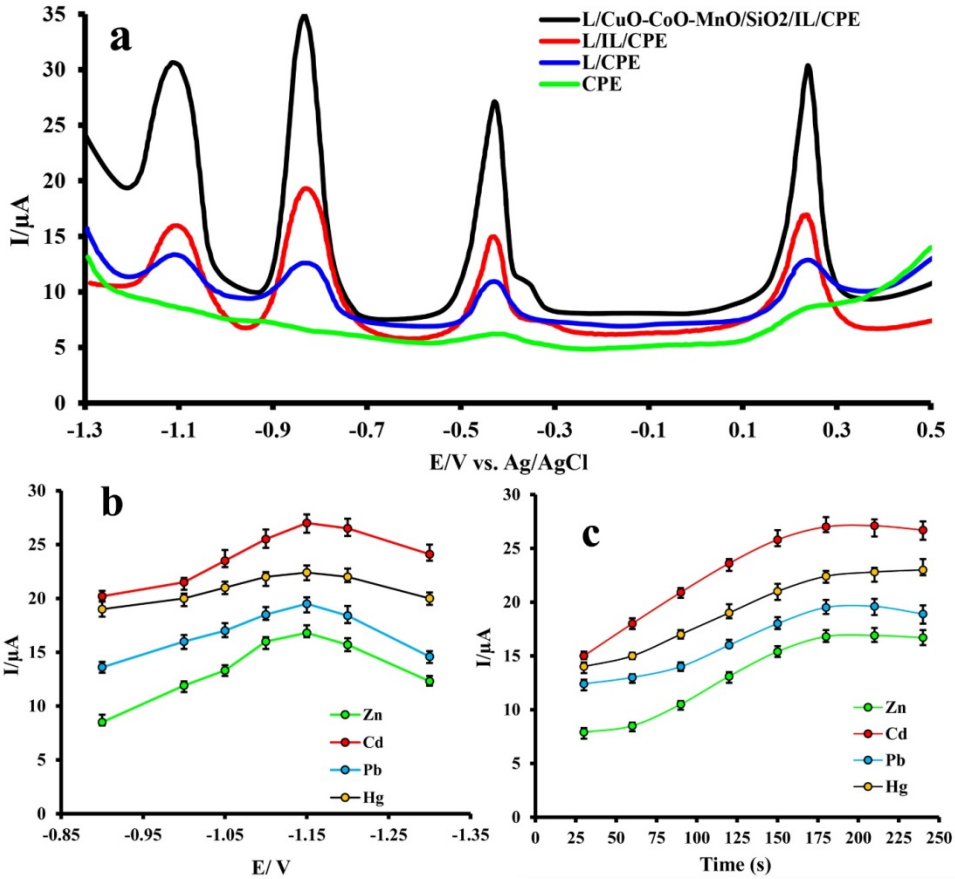

Fig. 2. (a) SWASV s of 5µM Hg(II), Cd(II), Pb(II) and Zn(II) in B-R buffer solution (pH 3.5) on the surface of CPE, L/CPE, L/IL/CPE, and L/CuO-CoO-MnO/SiO_2/IL/CPE (Condition: deposition potential= -1.15 v vs. Ag/AgCl, deposition time= 180s, Voltage step: 5 mV, Pulse amplitude: 110 mV, SW frequency: 50Hz and Resting time: 20 s); (b) Effect of deposition potential on the anodic stripping peak current for 5µM Hg(II), Cd(II), Pb(II) and Zn(II) in B-R buffer solution (pH 3.5) at L/CuO-CoO-MnO/SiO_2/IL/CPE; (c) Effect of deposition time on the anodic stripping peak current for 5µM Hg(II), Cd(II), Pb(II) and Zn(II) in B-R buffer solution (pH 3.5) at L/CuO-CoO-MnO/SiO_2/IL/CPE

The sharper with higher peak currents (I_{pa}) for the Hg(II) at 0.238, Pb(II) at -0.424, Cd(II) at -0.832 and Zn(II) -1.1 V vs. Ag/AgCl were obtained at the L/CPE and peak separations (ΔE_p) of 0.662, 408 and 0.268 vs. Ag/AgCl for Hg-Pb, Pb-Cd, and Cd-Zn, respectively. It can be seen that the ΔEp between obtained peaks is enough to the concomitant determination of the target heavy metal ions, but to achieve better detection limit

(DL) and sensitivity L/CPE was modified by IL. On the surface of IL/L/CPE, four well-defined and sharp peaks were observed with higher oxidation peak currents compared to L/CPE. Also, the Epa for the analytes has no changed at IL/L/CPE. These results propose that using IL can extremely increment the rates of the heavy metal ions preconcentration from the bulk solution to the surface of the working electrode. Furthermore, IL can improve the electron transfer rate between target ions and electrode surface, based on these two factors, the response of IL/L/CPE was better than L/CPE and CPE. In the absenteeism of target metal ions, the L/CuO-CoO-MnO/SiO_2/IL/CPE did not show any oxidation peaks in the electrochemical potential windows -1.3 – 0.5 V vs. Ag/AgCl.

Moreover, the currents at the L/CuO-CoO-MnO/SiO_2/IL/CPE have increased significantly in comparison to IL/L/CPE, which can be due to decrease the charge transfer resistance and increment the electrochemically active surface area. The I_{pa} for Hg(II), Cd(II), Pb(II) and Zn(II) were about 2.28, 2.54, 2.21 and 1.89 times more than IL/L/CPE, which may provide lower detection limits, high sensitivity and wide linear range. The peak shapes of Pb(II) were not symmetric, which it can be owing to the heterogeneous electrochemical process on the surface of the electrode [45]. Also, the observed shoulder at the right side of the oxidation peak of Pb(II) can be owing to the formation of Pb-Hg intermetallic compound in the accumulation step [46].

The response of L/CuO-CoO-MnO/SiO_2/IL/CPE can be affected by several factors such as kind of supporting electrolyte, the concentration of H^+ in the solution, deposition time and potential, and some instrumental parameters, so these parameters must be optimized to achieve the best response and efficiency of electrode.

3.4. Optimization of experimental parameters

3.4.1. Effect of supporting electrolyte and solution pH

Before the detection, the influence of different factors on the response of the electrode was investigated by using SWASV technique. The impact of different supporting electrolytes including KNO_3, $HClO_4$, acetate buffer solution, B-R buffer solution and phosphate buffer solution, on the determination of 5 μM at L/CuO-CoO-MnO/SiO_2/IL/CPE were studied. The best result, with three factors, include the highest oxidation striping peak currents, the best peak shape, and lowest background current, was achieved when the B-R buffer solution was used as supporting electrolyte.

Also, the impact of solution pH in the range of 2 to 11 on the response of using electrode was studied and obtained results show that the best pH for simultaneous determination of Hg(II), Cd(II), Pb(II) and Zn(II) was pH=3.5. In the pH above 6, noisy voltammograms were observed which could be due to the formation of hydroxide precipitates of heavy metal ions; however, the proton can compete with the heavy metal ions in make complex by L; therefore the currents in pH below 3.5 are lower than pH=3.5.

3.4.2. Optimization of deposition potential, deposition time and parameters of the electrochemical method

Deposition parameters are the most critical variables in the stripping analysis to achieve the lowest detection limit (DL) and highest sensitivity. The effect of accumulation potential on the currents in the range of -0.9 to -1.3 V *vs.* Ag/AgCl after 180 s deposition time in 0.1 M B-R buffer solution at pH=3.5 was studied, and the data are shown in Fig. 2b. With increasing the deposition potential to more negative values from -0.9 to -1.15 V *vs.* Ag/AgCl the oxidation stripping currents for all analytes growth and reached to the maximum value at -1.15 V *vs.* Ag/AgCl because the less cathodic potential was insufficient to reduce the metal ions. Differently, by employing the deposition potential more than -1.15 V *vs.* Ag/AgCl, the received response from the electrode has decreased significantly due to the generation of H_2. According to obtained data for achieving the maximum peak currents and in order to avoid deposition of other metal ions which may be present in real samples, the -1.15 V *vs.* Ag/AgCl was used as the optimal accumulation potential for the subsequent experiment.

In another study, the impact of different deposition times to find the best DL and sensitivity on the response of L/CuO-CoO-MnO/SiO_2/IL/CPE were investigated in 0.1 M B-R buffer solution at pH=3.5, and -1.15 v *vs.* Ag/AgCl applied as optimum deposition potential. The stripping oxidation currents for Hg(II), Cd(II), Pb(II) and Zn(II) have increased significantly while the longer deposition times were employed, however, after 180 s the currents reached a plateau because the modified electrode surface was saturated by adsorbed heavy metal ions (Fig. 2c). Thus, to earn both wide response range of the electrode and the best sensitivity for Hg(II), Cd(II), Pb(II) and Zn(II) determination the 180 s was chosen as the optimum deposition time.

In addition, in order to achieve the best result for electrochemical determination of the target heavy metal ions, the best peak shape, sensitivity and selectivity, instrumental parameters of SWV include Voltage step, Pulse amplitude, SW frequency and Resting time were optimized. The following settings for SWV technique are suggested: Voltage step: 5 mV, Pulse amplitude: 110 mV, SW frequency: 50Hz and Resting time: 20 s.

3.4.3. Analytical performance for Hg(II), Cd(II), Pb(II) and Zn(II)

Under the optimized chemical and method conditions, individual and concomitant determination of target heavy metal ions were recorded by SWASV in 0.1 M B-R buffer solution with pH=3.5 with concentrations increasing in the range of Hg: 0.0007-0.21 and 0.21-27 µM, Cd: 0.0007-0.21 and 0.21-27 µM, Pb: 0.0009-0.23 and 0.23-27 µM, Zn: 0.001-0.25 and 0.25-27 µM to evaluate the electrochemical performance.

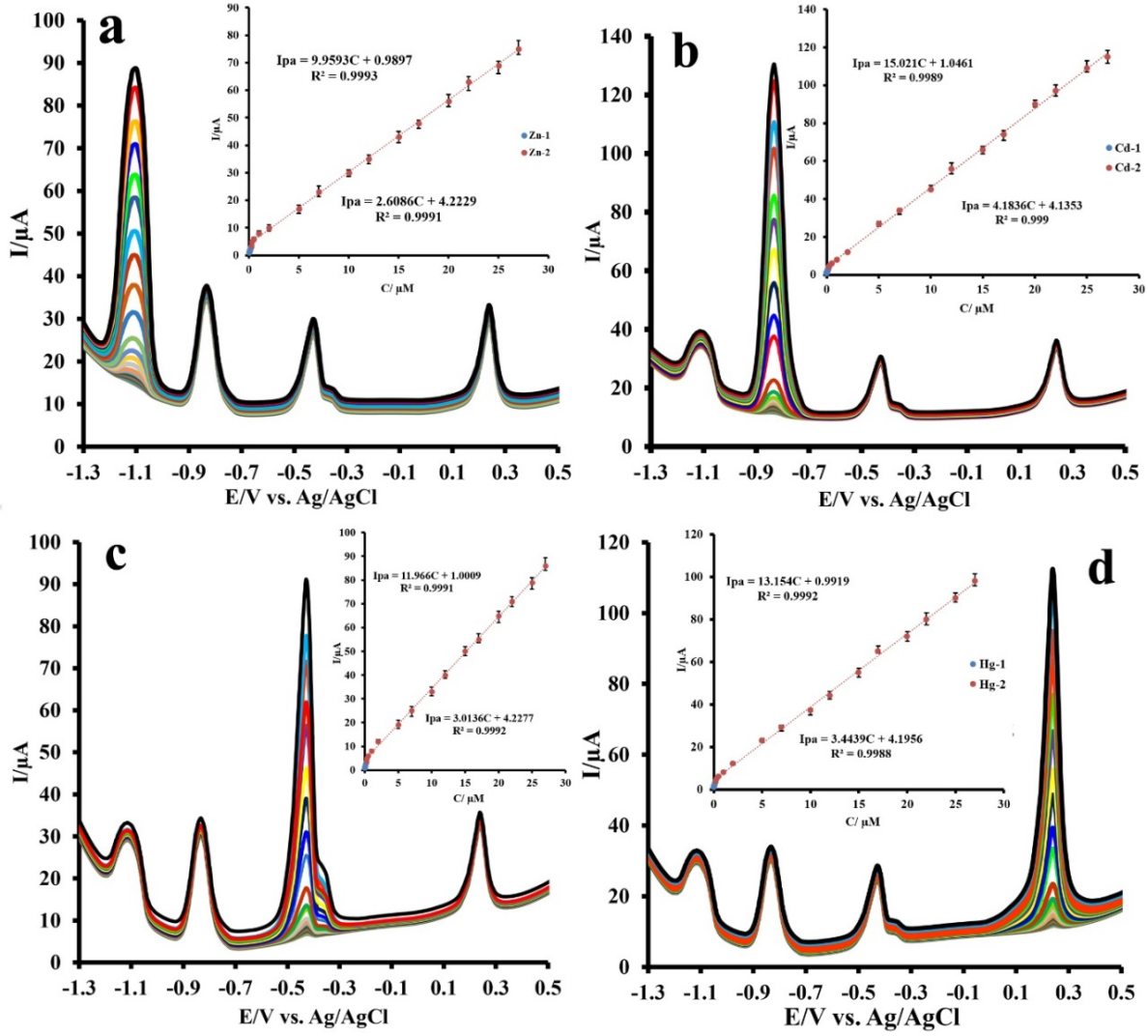

Fig. 3. SWASV using L/CuO-CoO-MnO/SiO_2/IL/CPE in B-R buffer solution (pH 3.5) containing different concentrations of (a) Zn(II), (b) Cd(II), Pb(II) and Hg(II) in the presence constant concentration (5µM) of other analytes (Condition: deposition potential= -1.15 v vs. Ag/AgCl, deposition time= 180s, Voltage step: 5 mV, Pulse amplitude: 110 mV, SW frequency: 50Hz and Resting time: 20 s). Inset shows the calibration plot of the anodic stripping peak currents as a function of each analyte concentrations

In the first experiment, under the optimized conditions, the anodic striping peak currents from SWASV of each analyte in the present of a constant amount of the three other analytes (5 µM) were proportional to concentrations (Fig. 3a-d) with the regression equation in the mentioned range of Hg: I_{pa} = 13.154C + 0.9919 (0.0007-0.21 µM, R^2 = 0.9992) and I_{pa} = 3.4439C + 4.1956 (0.21-27 µM, R^2 = 0.9988), Cd: I_{pa} = 15.021C + 1.0461 (0.0007-0.21 µM, R^2 = 0.9989) and I_{pa} = 4.1836C + 4.1353 (0.21-27 µM, R^2 = 0.999), Pb: I_{pa} = 11.966C + 1.0009 (0.0009-0.23 µM, R^2 = 0.9991) and I_{pa} = 3.0136C + 4.2277 (0.23-27 µM, R^2 =

0.9992), Zn: I_{pa} = 9.9593C + 0.9897 (0.001-0.25 µM, R^2 = 0.9993) and I_{pa} = 2.6086C + 4.2229 (0.25-27 µM, R^2 = 0.9991). It can be say that the current of analytes, which have constant concentration, were almost unchanged.

In other experiments, under the optimized experimental conditions include pH=3.5, deposition potential= -1.15 v vs. Ag/AgCl, deposition time= 180s, Voltage step: 5 mV, Pulse amplitude: 110 mV, SW frequency: 50Hz and Resting time: 20 s, the sensitivity and linear range of the L/CuO-CoO-MnO/SiO_2/IL/CPE for simultaneous determination of Hg(II), Cd(II), Pb(II) and Zn(II) were evaluated in B-R buffer solution (Fig. 4a). The obtained results represented that the plot of the oxidation stripping peak currents of Hg(II), Cd(II), Pb(II) and Zn(II) are accompanied by an increase in target heavy metal ions concentration in Fig. 4b and c by the following equations:

Hg(II)	0.0007-0.21 µM	I_{pa} = 13.022C + 0.9967	R^2 = 0.9992	Eq. 2
	0.21-27 µM	I_{pa} = 3.5367C + 3.9569	R^2 = 0.9987	Eq. 3
Cd(II)	0.0007-0.21 µM	I_{pa} = 14.722C + 1.0548	R^2 = 0.9991	Eq. 4
	0.21-27 µM	I_{pa} = 4.2823C + 3.6557	R^2 = 0.9989	Eq. 5
Pb(II)	0.0009-0.23 µM	I_{pa} = 11.496C + 1.0131	R^2 = 0.9989	Eq. 6
	0.23-27 µM	I_{pa} = 2.9783C + 4.4054	R^2 = 0.9988	Eq. 7
Zn(II)	0.001-0.25 µM	I_{pa} = 9.8742C + 0.9958	R^2 = 0.999	Eq. 8
	0.25-27 µM	I_{pa} = 2.5209C + 4.7967	R^2 = 0.9989	Eq. 9

Comparison between the slopes of calibration equations in the individual and simultaneous mode for each ion shows that there is no disturbance on the measurement of each ion on the determination of others because the slopes of equations for each element in both modes are approximately equal. The DLs were 3.019×10^{-4}, 3.445×10^{-4}, 2.407×10^{-4} and 5.134×10^{-4} µM for Hg (II), Cd (II), Pb (II) and Zn (II) respectively, based on $3S_b/m$ (m: slopes of calibration equations, S_b: the standard deviation of the voltammetric response of the blank solution, n= 7)

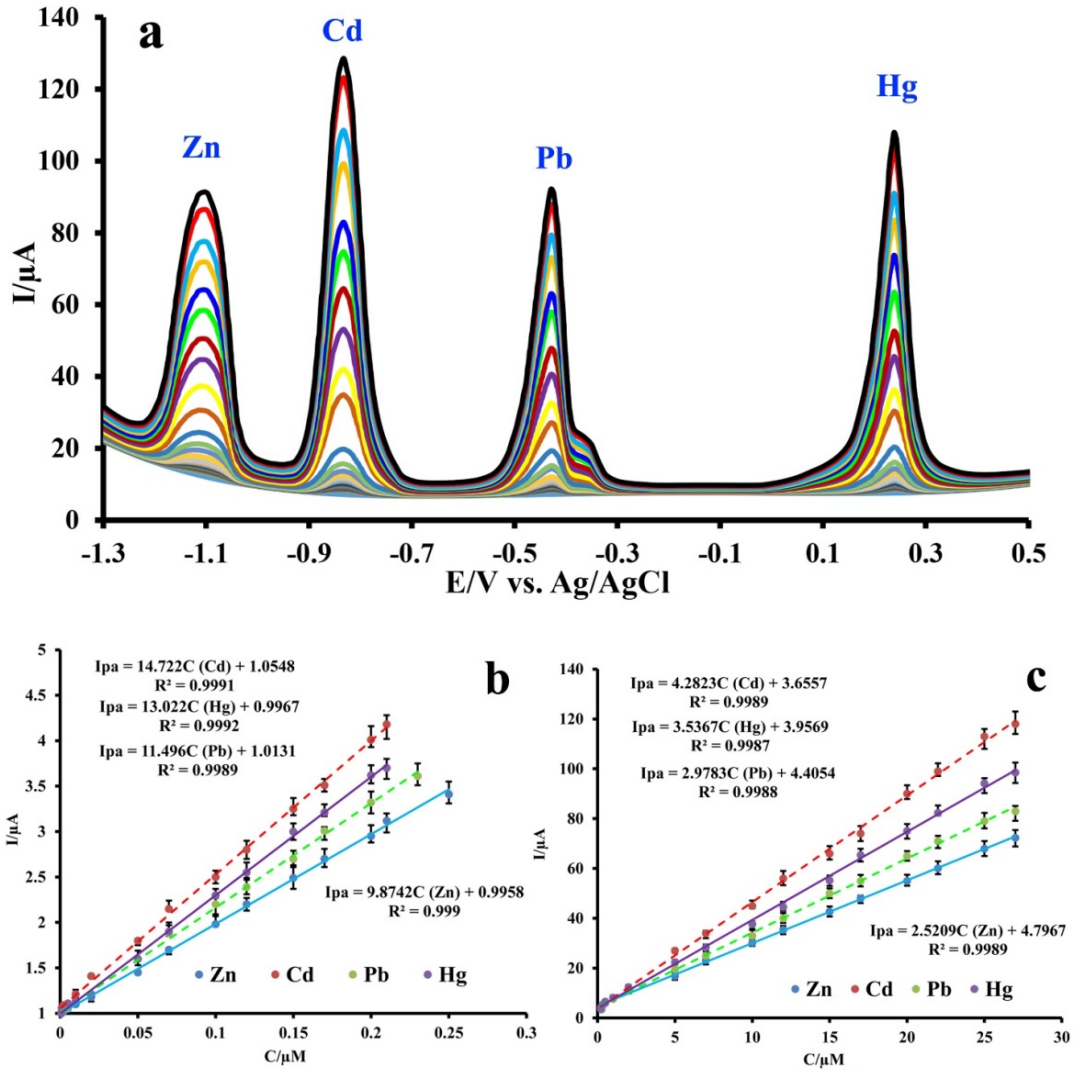

Fig. 4 (a) SWASV of different concentrations of Hg(II), Cd(II), Pb(II) and Zn(II) in in B-R buffer solution (pH 3.5) using L/CuO-CoO-MnO/SiO_2/IL/CPE and under optimum conditions; The calibration plot of the corrected electrochemical peak currents as a function of analytes concentrations in the range of (b) Hg: 0.0007-0.21 µM, Cd: 0.0007-0.21 µM, Pb: 0.0009-0.23 µM, Zn:0.001-0.25 µM (c) Hg: 0.21-27 µM, Cd: 0.21-27 µM, Pb: 0.23-27 µM, Zn: 0.25-27 µM

3.5. Selectivity, repeatability, reproducibility, and stability of the L/CuO-CoO-MnO/SiO_2/IL/CPE

The response of the prepared electrode was checked when the target ions were in the presence of some ions, which can potentially coexist in the various real sample. The selected species as interference elements were added into the in 0.1 M B-R buffer solution with pH=3.5 containing the 5 µM target heavy metal ions, and their effect on the anodic stripping peak currents were studied. The results illustrate that 200-fold for Cl^-, F^-, $SO4^{2-}$, K^+, Mn^{2+},

Li^+, Ca^{2+}, Mg^{2+}, Al^{3+}, NH_4^+, Cl^-, NO_3^-, SO_4^{2-}, PO_4^{3-}, and also Fe^{3+} could not change the obtained current of proposed electrode more than 5%. In addition, with the addition of Cu^{2+} to the solution of target analytes, a shoulder has appeared at -0.338 V Ag/AgCl, which can be due to Cu-Pb interaction [45]. The obtained data illustrates that this shoulder can affect the oxidation stripping current and DL of Pb(II) when it was more than 35-fold.

The fabricated L/CuO-CoO-MnO/SiO_2/IL/CPE is appraised by repetitive determination of 5 μM of Hg(II), Cd(II), Pb(II) or Zn(II) under optimized chemical and instrumental factors to study its repeatability. The relative standard deviation (RSD%) from five successive determination using a single modified electrode was measured to be 2.6% for Hg(II), 3.2% for Cd(II), 3.6% for Pb(II) and 3.4% for Zn(II).

The reproducibility of L/CuO-CoO-MnO/SiO_2/IL/CPE was appraised by analyzing a solution containing 5 μM the heavy metal ions with ten independently prepared sensors based on the similar construction method. The presented electrode illustrates an appropriate precision with RSD% of 3.8, 4.2, 4.0 and 3.5% for Hg(II), Cd(II), Pb(II) and Zn(II) respectively.

After each measurement, the L/CuO-CoO-MnO/SiO_2/IL/CPE was kept in the refrigerator at 4 °C. Every day the voltammetric response for determination of 5 μM the heavy metal ions under optimal condition was recorded. The oxidation currents diminished Zn(II): 1.7%, Pb(II): 2.9% and Cd(II): 3.2% and increased Hg(II): 4.3% of relative to the initial amount after 30 days, denoting that the proposed sensor has acceptable stability.

These obtained values of RSD% indicate good repeatability and reproducibility of L/CuO-CoO-MnO/SiO_2/IL/CPE for the simultaneous measurement of the Hg(II), Cd(II), Pb(II) and Zn(II).

3.6. Analytical application for real samples

To investigate the applicability of the suggested method in real samples, such as tap water and river water, were tested. The collected tap and river water samples were filtered through a standard 0.45 μm filter and used without another pretreatment.

The results of this test are summarized in Table 1, with the percentage of recoveries of the spiked samples ranged from 98.1% to 102.7%. Also, the obtained response of the electrochemical determinations accorded very well with those obtained by AAS, which corroborated the accuracy and reliability of the proposed method.

It was evident that the L/CuO-CoO-MnO/SiO_2/IL/CPE could be successfully applied for the simultaneous measurements of Hg(II), Cd(II), Pb(II) and Zn(II) in the chosen real samples.

Table 1. Results for Zn(II), (b) Cd(II), Pb(II) and Hg(II) determination (nM) in Tap water and River water samples obtained under the optimum conditions (n = 5)

Sample	Analyte	Added (nM)	Found (nM)	RSD (%)	Recovery (%)	AAS*
Tap water	Hg(II)	0.0	0.92	3.2	-	0.91
		10.0	11.04	3.1	101.2	11.09
	Pb(II)	0.0	29.54	3.3	-	29.84
		30.0	60.35	2.8	102.7	60.34
	Cd(II)	0.0	2.06	3.2	-	2.11
		10.0	11.87	2.9	98.1	11.96
	Zn(II)	0.0	421.51	2.5	-	425.16
		200.0	619.64	3.4	99.0	624.48
River water	Hg(II)	0.0	10.47	3.3	-	10.36
		10.0	20.32	2.9	98.5	20.12
	Pb(II)	0.0	131.95	2.2	-	130.88
		100.0	233.14	2.8	101.2	231.00
	Cd(II)	0.0	50.85	2.6	-	48.97
		50.0	100.09	3.2	98.5	103.18
	Zn(II)	0.0	273.21	3.4	-	276.61
		200.0	476.54	3.0	101.7	485.43

AAS : Atomic Absorption Spectrometry

The values in parentheses are RSD% based on five replications.

4. CONCLUSION

In brief, an unprecedented chemically modified electrochemical sensor has been developed and victoriously applied for the individual, and concomitant determination of some

heavy metal ions include Hg(II), Cd(II), Pb(II) and Zn(II) in the wide linear range by SWASV for the first time. The effective parameters were optimized, and the linear ranges were obtained as Hg: 0.0007-0.21 and 0.21-27 µM, Cd: 0.0007-0.21 and 0.21-27 µM, Pb: 0.0009-0.23, 0.23-27 µM, Zn:0.001-0.25, 0.25-27 µM with low DLs of 3.019×10^{-4}, 3.445×10^{-4}, 2.407×10^{-4} and 5.134×10^{-4} µM for Hg(II), Cd(II), Pb(II) and Zn(II), respectively. The selectivity investigation shows that the suggested method is highly selective toward target ions. In addition, L/CuO-CoO-MnO/SiO_2/IL/CPE has high stability, repeatability and reproducibility. Further, the suggested method was used successfully to the measurement of the heavy metal ions in tap and river water, which obtained data and percentage of recovery show that L/CuO-CoO-MnO/SiO_2/IL/CPE is trustworthy for using in routine analysis in the laboratory.

REFERENCES

[1] H. Karimi-Maleh. F. Karimi. M. Rezapour. M. Bijad. M. Farsi. A. Beheshti, and S.A. Shahidi, Curr. Anal. Chem. 15 (2019) 410.

[2] A. Mirabi. A. S. Rad. F. Divsalar, and H. Karimi-Maleh, Arabian J. Sci. Eng. 43 (2018) 3547.

[3] M. C. Nayak. A. M. Isloor. B. Lakshmi. H. M. Marwani, and I. Khan, Arabian J. Chem. 13 (2020) 4661.

[4] B. J. Alloway, Heavy metals in soils: trace metals and metalloids in soils and their bioavailability, Springer Science & Business Media (2012).

[5] M. Patra, and A. Sharma, Bot. Rev. 66 (2000) 379.

[6] V. K. Gupta. M. L. Yola. N. Atar. Z. Ustundağ, and A. O. Solak, Electrochim. Acta 112, (2013) 541.

[7] Y.-H. Li. Z. Di. J. Ding. D. Wu. Z. Luan, and Y. Zhu, Water Res. 39 (2005) 605.

[8] E. Liu. L. Pimpin. M. Shulkin. S. Kranz. C. Duggan. D. Mozaffarian, and W. Fawzi, Nutrients 10 (2018) 377.

[9] S. Tubek, Biol. Trace Elem. Res. 119 (2007) 1.

[10] X. Han. Z. Meng. H. Zhang, and J. Zheng, Microchim. Acta 185 (2018) 274.

[11] F. Long. A. Zhu. H. Shi. H. Wang, and J. Liu, Sci. Rep. 3 (2013) 2308.

[12] S. Anandhakumar. J. Mathiyarasu. K. L. N. Phani, and V. Yegnaraman, Am. J. Anal. Chem. 2, (2011) 470.

[13] B. Kaur. R. Srivastava, and B. Satpati, New J. Chem. 39 (2015) 5137.

[14] A. Babaei, and A. R. Taheri, Sens. Actuators B 176 (2013) 543.

[15] M. Hasanzadeh. N. Shadjou, and E. Omidinia, J. Neurosci. Methods 219 (2013) 52.

[16] H. Karimi-Maleh, and O. A. Arotiba, J. Colloid Interface Sci. 560 (2020) 208.

[17] H. Karimi-Maleh. C. T. Fakude. N. Mabuba. G. M. Peleyeju, and O. A. Arotiba, J. Colloid Interface Sci. 554 (2019) 603.

[18] S. Tajik. N. Akbarzadeh-Torbati. M. Safaei, and H. Beitollahi, Int. J. Electrochem. Sci. 14 (2019) 4361.

[19] Y. Li. Y. Ji. B. Ren. L. Jia. G. Ma, and X. Liu, Mater. Res. Bull. 109, (2019) 240.

[20] A. Shams, and A. Yari, Sens. Actuators B 286 (2019) 131.

[21] A. Afkhami. T. Madrakian. S. J. Sabounchei. M. Rezaei. S. Samiee, and M. Pourshahbaz, Sens. Actuators B 161 (2012) 542.

[22] F. Tahernejad-Javazmi. M. Shabani-Nooshabadi, and H. Karimi-Maleh, Composites, Part B 172 (2019) 666.

[23] M. Miraki. H. Karimi-Maleh. M. A. Taher. S. Cheraghi. F. Karimi. S. Agarwal, and V. K. Gupta, J. Mol. Liq. 278 (2019) 672.

[24] H. Karimi-Maleh. M. Sheikhshoaie. I. Sheikhshoaie. M. Ranjbar. J. Alizadeh. N. W. Maxakato, and A. Abbaspourrad, New J. Chem. 43 (2019) 2362.

[25] V. R. R. Bernardo-Boongaling. N. Serrano. J. J. García-Guzmán. J. M. Palacios-Santander, and J. M. Díaz-Cruz, J. Electroanal. Chem. 847, (2019) 113184 .

[26] E. Afsharmanesh. H. Karimi-Maleh. A. Pahlavan, and J. Vahedi, J. Mol. Liq. 181 (2013) 8.

[27] S. Cheraghi. M. A. Taher, and H. Karimi-Maleh, J. Food Compos. Anal. 62 (2017) 254.

[28] R. Sadeghi. H. Karimi-Maleh. A. Bahari, and M. Taghavi, Phys. Chem. Liq. 51 (2013) 704.

[29] T. Jamali. H. Karimi-Maleh, and M. A. Khalilzadeh, LWT-Food Sci. Technol. 57 (2014) 679.

[30] H. Karimi-Maleh. P. Biparva, and M. Hatami, Biosens. Bioelectron. 48 (2013) 270.

[31] B. Šljukić. C. E. Banks, and R. G. Compton, Nano Lett. 6 (2006) 1556.

[32] Z. Zang. A. Nakamura, and J. Temmyo, Opt. Express 21 (2013) 11448.

[33] S. Harish. M. Navaneethan. J. Archana. S. Ponnusamy. C. Muthamizhchelvan, and Y. Hayakawa, Mater. Lett. 139 (2015) 59.

[34] J. Liu. L. Jiang. B. Zhang. J. Jin. D. S. Su. S. Wang, and G. Sun, ACS Catal. 4 (2014) 2998.

[35] M. Zheng. H. Zhang. X. Gong. R. Xu. Y. Xiao. H. Dong. X. Liu, and Y. Liu, Nanoscale Res. Lett. 8 (2013) 166.

[36] J. Tashkhourian, and S. Ghaderizadeh, Russ. J. Electrochem. 50 (2014) 959.

[37] Y.Q. Zhao. Y.H. Liang. X.Z. Zhao. Q. Y. Jia, H.S. Li, Prog. Nat. Sci.: Mater. Int. 21, (2011) 330.

[38] Z. Shaghaghi, Spectrochim. Acta Part A 131 (2014) 67.

[39] B. M. Quinn. Z. Ding. R. Moulton, and A. J. Bard, Langmuir 18 (2002) 1734.

[40] A. F. Mulaba-Bafubiandi. H. Karimi-Maleh. F. Karimi, and M. Rezapour, J. Mol. Liq. 285 (2019) 430.

[41] Y. Zhao. X. Zhao. M. Zhang, and Q. Jia, Microporous Mesoporous Mater. 261 (2018) 220.

[42] V. V. Thekkae Padil, and M. Černík, Int. J. Nanomed. 8 (2013) 889.

[43] H.T. Zhang, and X. H. Chen, Nanotechnology 16 (2005) 2288.

[44] M. Criado. A. Fernández-Jiménez, and A. Palomo, Microporous Mesoporous Mater. 106 (2007) 180.

[45] Z. Zhai. N. Huang. H. Zhuang. L. Liu. B. Yang. C. Wang. Z. Gai. F. Guo. Z. Li, and X. Jiang, Appl. Surf. Sci. 457 (2018) 1192.

[46] Y. Wei. C. Gao. F.-L. Meng. H.H. Li. L. Wang. J.H. Liu, and X.J. Huang, J. Phys. Chem. C 116 (2011) 1034.